https://doi.org/10.5194/tc-2022-136
Preprint. Discussion started: 8 July 2022
© Author(s) 2022. CC BY 4.0 License.

The Cryosphere Discussions

Impact of icebergs on the seasonal submarine melt of Sermeq Kujalleq

Karita Kajanto[1], Fiammetta Straneo[2,3], and Kerim Nisancioglu[1]

[1]Department of Earth Science, University of Bergen and Bjerknes Centre for Climate Research, Bergen, Norway
[2]Scripps Institution of Oceanography, UCSD, CA, USA
[3]Geophysical Institute, University of Bergen and Bjerknes Centre for Climate Research, Bergen, Norway

Correspondence: Karita Kajanto (karita.kajanto@uib.no)

Abstract. The role of icebergs in narrow fjords hosting marine terminating glaciers in Greenland is poorly understood, even though icebergs provide a substantial freshwater flux that can exceed the subglacial discharge. Iceberg melt is distributed at depth, contributing to fjord stratification, thus impacting melt and dynamics of the glacier front. We model the high-silled Ilulissat Icefjord in Western Greenland with the MITgcm ocean model, using the IceBerg package to study the effect of icebergs on fjord properties, and compare our results with available observations from 2014. We find the subglacial discharge plume to be the primary driver of the seasonality of circulation, glacier melt and iceberg melt. Icebergs are necessary to include to correctly understand the properties of Ilulissat Icefjord, since they modify the fjord in three main ways: First, icebergs cool and freshen the water column within their vertical extent; Second, icebergs depress the neutral buoyancy depth of the plume and the outflow route of glacially modified water; Third, icebergs modify the deep basin, below their vertical extent, due to both increased entrainment of glacially modified water into the fjord, and iceberg modification of the incoming ambient water. Furthermore, the depressed neutral buoyancy depth of the plume limits melt to the deep section of the front of Sermeq Kujalleq (Jakobshavn Isbræ) even during peak summer, and thus promotes undercutting. We postulate that the impact of icebergs on the neutral buoyancy depth of the plume is a key mechanism connecting iceberg melange and glacier calving, independent of mechanical support.

1 Introduction

Marine-terminating outlet glaciers contribute to approximately half of the mass loss from the Greenland Ice Sheet, and are sensitive to changes in external forcing (Slater et al., 2019; Straneo et al., 2019; Catania et al., 2020; Goelzer et al., 2020). Glaciers terminating in a narrow fjord are controlled by the fjord geometry (Åkesson et al., 2018; Frank et al., 2021) and fjord stratification (Slater et al., 2016; De Andrés et al., 2020). The ice-ocean interface remains the main source of uncertainty in the sea level contribution estimates from the Greenland ice sheet (Goelzer et al., 2020), despite significant effort through modelling, observations and satellite monitoring (Straneo et al., 2019; Catania et al., 2020). The key uncertainties of the field, such as subglacial discharge, shape of the plume and calving have been thoroughly discussed in Straneo et al. (2019). Despite the uncertainties, there is accumulating evidence of the ocean driving retreat of marine-terminating glaciers, although individual glaciers in Greenland can have very different responses due to local features (Slater et al., 2019; Catania et al., 2020).

https://doi.org/10.5194/tc-2022-136
Preprint. Discussion started: 8 July 2022
© Author(s) 2022. CC BY 4.0 License.

The Cryosphere Discussions
Open Access
EGU

Many of the fast-flowing, marine-terminating glaciers in Greenland discharge the majority of their ice through calving of icebergs (Mouginot et al., 2019; Wood et al., 2021). Observations indicate a close connection between dense iceberg melange in front of the glacier and glacier calving. This connection has been interpreted to be due to mechanical support provided by a rigid iceberg melange that suppresses calving (Joughin et al., 2008; Amundson et al., 2010; Burton et al., 2018; Joughin et al., 2020). Meanwhile, there is accumulating observational evidence that icebergs are an important contributor to fjord stratification, and that much of the transformation of ocean waters due to ice-ocean exchanges takes place along the fjord — due to, for example, icebergs — rather than directly at the glacier terminus (Moon et al., 2018; Mortensen et al., 2020; Muilwijk et al., 2021). Estimates for rapidly calving glaciers indicate that icebergs can be a larger freshwater source than subglacial discharge (Enderlin et al., 2016; Moon et al., 2018), and take up the majority of the heat used for melting in a such fjord (Davison et al., 2020). Thus, irrespective of a mechanical connection, iceberg-modification of the water column provides a mechanism that enables icebergs to potentially impact the glacier front.

We investigate how icebergs modify the stratification and circulation in the fjord, and the implications of this modification to the glacier front. We construct a model of the Ilulissat Icefjord, which is a high-silled, rapidly calving and iceberg-congested fjord in Western Greenland. We use the IceBerg toolbox (Davison et al., 2020) within the MITgcm ocean model to include the impact of icebergs, and to investigate and quantify their impact on fjord stratification and circulation. We prescribe the seasonal evolution of the subglacial discharge from winter to peak summer, and characterize the role icebergs play at each phase of the discharge season. We study the sensitivity of the model to the distribution and draft of the icebergs, and the configuration of the subglacial discharge plume. The results are compared with available observational data from the fjord. Finally, we summarize and discuss the impact the icebergs have on the stability of the glacier, and consider the implications for the future response of Sermeq Kujalleq in a warming climate.

2 Ilulissat Icefjord

Ilulissat Icefjord (also known as Kangia) is a 50 km long East–West oriented fjord at the eastern edge of Disko Bay, Western Greenland (also known as Qeqertarsuup tunua) (Fig. 1). The terminus of the fastes flowing glacier of Greenland, Sermeq Kujalleq (also known as Jakobshavn Isbræ), is located in the eastern end of the Ilulissat Icefjord. Sermeq Kujalleq is the most rapidly calving glacier of the Greenland Ice Sheet: during the high-discharge years of 2004–2014 its calving rate was estimated to reach over 70 Gt/a in the height of summer (Bondzio et al., 2017), leaving the fjord clogged with icebergs. The sill at the mouth of Ilulissat Icefjord is relatively high — appr. 250 m — compared to the fjord depth, which is 700–800 m (Morlighem et al., 2017). Iceberg drafts can reach down to 400–500 m (Enderlin et al., 2016), causing these large icebergs to spend substantial amounts of time on the sill, before melting enough to exit over the sill into Disko Bay. This dense melange makes the fjord difficult to study, as it is inaccessible by boat most of the year, however expendable CTD-campaigns (XCTD) and instrumented seals provide observational data for peak and late summer (Gladish et al., 2015; Mernild et al., 2015; Fenty, I. et al., 2016; Beaird et al., 2017).

https://doi.org/10.5194/tc-2022-136
Preprint. Discussion started: 8 July 2022
© Author(s) 2022. CC BY 4.0 License.

The Cryosphere Discussions

Observations indicate that the fjord can be described with three different layers: surface layer (0–50 m), intermediate layer (50–300 m) and the deep basin (300–800 m), see Fig. 2b. The dominant characteristic of the surface layer is that it is cold and fresh, due to melt of the iceberg melange and a smaller contribution from surface runoff (Gladish et al., 2015; Mernild et al., 2015; Beaird et al., 2017; Mojica et al., 2021). The intermediate layer is a weakly stratified layer of glacially modified water (GMW), where the lower portion of the large icebergs resides (Beaird et al., 2017; Mojica et al., 2021). The deep basin is below the extent of most icebergs, and contains the warmest and most saline water in the fjord (Gladish et al., 2015; Mernild et al., 2015; Beaird et al., 2017; Mojica et al., 2021). There is little information on the seasonality in the fjord (Mernild et al., 2015), but the conventional idea is that basin water renewal by warm water over the sill takes place only during summer and is driven by the subglacial discharge plume (Gladish et al., 2015; Carroll et al., 2017).

The high sill of the Ilulissat Icefjord acts as a barrier in both directions, isolating the basin from the warmest and most saline water in Disko Bay, while blocking large icebergs from leaving the fjord. Both Gladish et al. (2015) and Beaird et al. (2017) find a sharp gradient in the surface layer properties at the sill, as the cold and fresh surface conditions in the fjord switch to the relatively warm summer conditions of Disko Bay. Seasonal profiles from Disko Bay, close to Qeqertarsuaq in Disko Island, roughly 100 km west from the Ilulissat Icefjord, show a strong seasonal signal, reaching down to 300 m depth, with significant warming and freshening during the summer, and slow cooling during winter (Fig. S1) (Greenland Ecosystem Monitoring, 2020). Summer profiles obtained in front of the sill demonstrate a similar strong summer surface warming (Fig. S1) (Beaird et al., 2017).

3 Methods

We use the Massachusetts Institute of Technology general circulation model, MITgcm, which solves the incompressible Navier-Stokes equations with finite volume methods (Marshall et al., 1997). We use an idealized, hydrostatic, high-silled fjord setup illustrated in Fig. 2, based on the Ilulissat Icefjord. The domain is a rectangular East–West oriented fjord that has a high sill at the fjord entrance and a vertical glacier front at the eastern end. The domain is 50 km~~'s~~ long, 8.5 km wide, and the sill is located at 5 km. The fjord is 700 m deep, the sill 250 m deep and the area in front of the sill representing Disko Bay 400 m. Grid resolution is 312.5*400*10 m. Even though the model is three dimensional, we do not consider Coriolis force, and use the third dimension primarily for icebergs and plume width considerations. We run the model for three months with winter conditions, and then run the model for 30 days with each monthly conditions (See Fig. S2).

The vertical glacier front is represented with the MITgcm IcePlume package (Cowton et al., 2015) that computes melt from the glacier front both with and in the absence of a subglacial discharge plume. The subglacial discharge outlet width — hereafter called plume width — is a key parameter of the model, since it contributes to the melt rate and neutral buoyancy depth (Jenkins, 2011). It is also a key uncertainty of our model, which we will discuss further in the sensitivity experiments in Section 4.4. In 1985, the base of the floating tongue of Sermeq Kujalleq of the time, showed a single wide channel Motyka et al. (2011). The front has retreated more than 10 km since then, and is now vertical, with two branches, although the southern branch is likely a much larger contributor. A large volume of surface runoff, as in the Sermeq Kujalleq catchment, does suggest

https://doi.org/10.5194/tc-2022-136
Preprint. Discussion started: 8 July 2022
© Author(s) 2022. CC BY 4.0 License.

The Cryosphere Discussions
Open Access
EGU

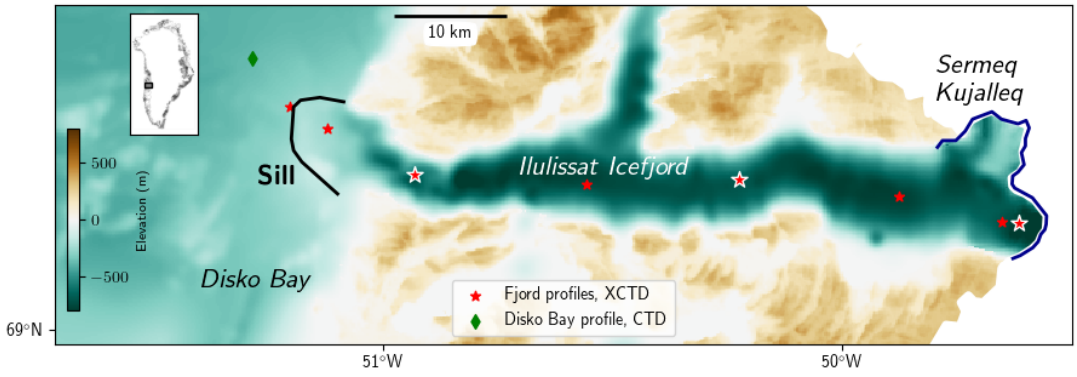

Figure 1. Map of Ilulissat Icefjord, indicating the sill (black line) and present day Sermeq Kujalleq front location (blue line). XCTD profile locations marked with red stars and CTD profile location used for boundary condition marked with a green diamond, all obtained in August 2014 (Beaird et al., 2017). Next-to-glacier, mid-fjord and close-to-sill profiles used in result plots are marked with a white outline. Bathymetry and topography are from BedMachine v3 (Morlighem et al., 2017).

a high degree of subglacial channeling, and thus a narrow plume (Cuffey and Paterson, 2010). However, Jackson et al. (2017) suggest that plumes with a width of several hundred meters are a better match to the observations than a point-source plume. Cavanagh et al. (2017) find that large portions of the surface runoff drain through both shear margins relatively close to the front, which suggests that there could be subglacial discharge beneath whole of the fast-flowing southern branch of the glacier.

Here, we choose a 1.2-km-wide sheet plume (Jenkins, 2011) as our default (Indicated with 'P' in experiments *IBP*, *NoIBP*, *IB200P* and *IB400P* in Table 1). For simplicity, the plume width is kept constant during each experiment, although Cook et al. (2021) show that for Store glacier, slightly further north along the west coast of Greenland, plume width can vary significantly during the year due to the evolution of the subglacial drainage system. To account for uncertainty in the plume width, we run sensitivity experiments with two additional plume widths: a wide plume of 4 km (*IB200WP*, *IBWP* and *IB400WP* in Table 1) and a narrow plume of 400 m (*IB200NP*, *IBNP* and *IB400NP* in Table 1). The wide plume corresponds to a situation where there is subglacial discharge along the whole southern branch of the glacier's calving front, while the narrow plume assumes that all runoff is routed into a single subglacial channel. All plumes are seasonal, with a bell-shaped discharge rate commencing in May and peaking in August. We assume peak subglacial discharge to take place in August, since surface runoff tends to peak around ~~in~~ Mid-July (Noël et al., 2019). The maximum volume flux of 1200 $m^3\ s^{-1}$ might be slightly underestimated for Sermeq Kujalleq, as Enderlin et al. (2016) estimate that the peak might reach up to 1200–1300 $m^3\ s^{-1}$. This uncertainty is nevertheless small compared to the uncertainty of the plume width.

https://doi.org/10.5194/tc-2022-136
Preprint. Discussion started: 8 July 2022
© Author(s) 2022. CC BY 4.0 License.

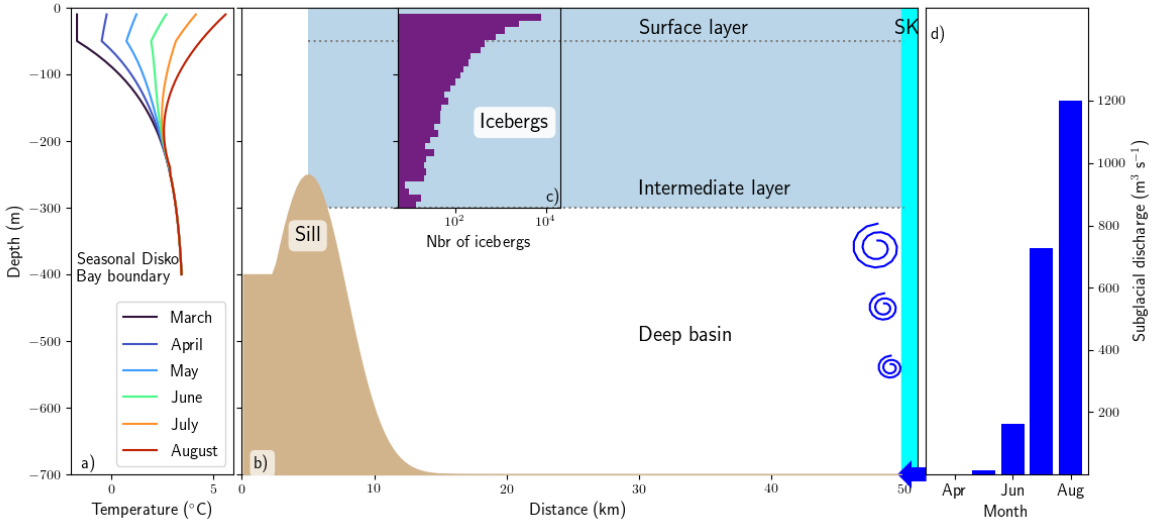

Figure 2. Model domain and forcings: a) Disko Bay temperature boundary condition from March to August. b) 2D-section of the model domain, grey shading indicates iceberg extent, dotted lines separate vertical layers used in describing results and the vertical pale blue block indicates the vertical front of Sermeq Kujalleq ('SK'). c) Number of icebergs of each depth at 10 m intervals. d) Monthly subglacial discharge forcing.

We choose to impose no separate surface forcing in the fjord, simiar to Gladish et al. (2015) and Davison et al. (2020), and assume that iceberg melt provides the dominant surface forcing and somewhat disconnects the fjord from atmospheric forcing. We also ignore the contribution from surface runoff, which we expect to mainly have an effect on the surface salinity in the fjord (Mernild et al., 2015). However, the summer warming and freshening of the fjord surface due to atmospheric forcing and runoff is accounted for by the Disko Bay boundary forcing: in the absence of icebergs, surface conditions in the fjord will follow those of Disko Bay. In the model, the western Disko Bay boundary is restored to temperature and salinity profiles, using a sponge layer of the OBCS package (Fig. 2a). The restoration timescale within the sponge layer ranges from is 17 hours on the outer boundary up to 1 month on the inner boundary, to ensure a smooth change of the ambient conditions (See Fig. S2). The winter boundary condition replicates observed profiles from Disko Bay (Greenland Ecosystem Monitoring, 2020) (see Fig. S1), while the summer profile replicates a CTD profile taken in Disko Bay, outside of the sill (Beaird et al., 2017) (green diamond in Fig. 1). Monthly boundary condition profiles are created by interpolating linearly between winter and summer profiles (Figs. 2a). However, we adjust temperature and salinity at sill depth to values observed at depth in the fjord (Beaird et al., 2017), and assume seasonality applies only above sill depth (Fig. S1). We initialize the fjord above sill depth with the winter profile, and constant temperature and salinity below sill depth, leading to no density gradient over the sill. We do not include sea ice formation, since we do not expect it to play a big role in spring and summer.

https://doi.org/10.5194/tc-2022-136
Preprint. Discussion started: 8 July 2022
© Author(s) 2022. CC BY 4.0 License.

The Cryosphere Discussions
Open Access
EGU

We implement iceberg forcing with the IceBerg package of MITgcm, presented in Davison et al. (2020). In this package, the fjord is filled with a randomly created block iceberg distribution following a power law of exponent -2.1, derived for Ilulissat Icefjord icebergs (Enderlin et al., 2016). We define the minimum and maximum iceberg depth and the surface area coverage. Melt and negative salinity flux are then computed from each iceberg face, similar to the sub-grid approach of Cowton et al. (2015), resulting in cell-averaged fluxes that force the ocean model. The effect of drift on melt rate is taken into account by considering the flow field in each computational cell with respect to the iceberg face orientation. The iceberg distribution remains fixed during the calculation, and the volume they uptake is reduced from the volume of each computational cell occupying icebergs. Other physical aspects, such as iceberg size decrease due to melt, or the sub-grid scale flow network icebergs create, are not included.

Enderlin et al. (2016) find for Ilulissat Icefjord that there often is a significant number of icebergs with estimated draft deeper than 200 m, but rarely many icebergs with drafts deeper than 400 m. Our default iceberg distribution covers 60% of the surface area of the fjord from the highest point of the sill to the glacier (grey area in Fig. 2b), with an iceberg-depth distribution from 10–300 m (Fig. 2c, experiments *IBP*, *NoIBP*, *IBWP* and *IBNP* in Table 1). To account for uncertainty in the iceberg distribution, we run two sets of sensitivity experiments with deeper and shallower icebergs (Fig. 10c). The deeper iceberg distribution has a maximum depth of 400 m and a high surface coverage of 90%, which is needed to fit the power law because deeper icebergs mean also more small icebergs (*IB400WP*, *IB400P* and *IB400NP* in Table 1). The shallow distribution has a maximum depth of 200 m and a surface coverage of 60%, leading to a larger number of small icebergs than in the default distribution (*IB200WP*, *IB200P* and *IB200WP* in Table 1). For a comperehensive list of all model parameters, see Table S1.

Table 1. Experiment naming and key parameters

Model name	IB max depth (m)	IB surface coverage (%)	Plume width (m)
Control without icebergs			
NoIBP	-		1200
Ilulissat Icefjord with icebergs			
IBP	300	60	1200
Sensitivity experiments			
IB200P	200	60	1200
IB400P	400	90	1200
IBNP	300	60	400
IBWP	300	60	4000
IB200NP	200	60	400
IB200WP	200	60	4000
IB400NP	400	90	400
IB400WP	400	90	4000

https://doi.org/10.5194/tc-2022-136
Preprint. Discussion started: 8 July 2022
© Author(s) 2022. CC BY 4.0 License.

The Cryosphere Discussions
Open Access
EGU

4 Results

We run our idealized Ilulissat Icefjord model, *IBP*, with monthly varying Disko Bay temperature and salinity, monthly increasing subglacial discharge, and a constant iceberg distribution (See Fig. 2). We compare this to a control experiment with no icebergs, *NoIBP* — otherwise identical to *IBP* — to investigate the impact icebergs have on fjord properties, circulation and glacier melt rate. Our experiments start from the prescribed winter conditions of the fjord (Fig. 2a), before the onset of Disko Bay surface warming and the increase in subglacial discharge, and we present results at the end of each month.

4.1 Seasonality without icebergs

We consider first the seasonality in Ilulissat Icefjord in the control experiment, *NoIBP*, without icebergs but including the plume. Above the sill, winter conditions in the fjord are dominated by the cold Disko Bay boundary condition. Below the sill, properties remain constant since there is no circulation in the deep basin (Figs. 3a and 4a). In the model, spring starts in April with a warming and freshening in Disko Bay (Figs. 2a, S1). Warming in Disko Bay progresses throughout spring, increasing the surface temperature in the fjord (Fig. 3a–e). In May, the runoff season starts with a small subglacial discharge (Fig. 2d). This subglacial discharge creates a buoyant plume that ascends vertically along the glacier front, until it reaches neutral buoyancy relative to the fjord water properties (red lines in Fig. 4b–e, Fig S4). After reaching the neutral buoyancy depth, the high vertical velocity transports the plume higher, further mixing with the fjord water, until the plume transforms to horizontal outflow of GMW (black arrows in Figs. 3 and 4). In May, the GMW outflow takes place at 230 m depth, partly exiting over the sill, partly mixing back into the basin (Fig. 4a). This mixing back into the deep basin at the sill is defined as sill-driven reflux in Hager et al. (2022).

As the subglacial discharge ~~volume~~ increases through June and July, the plume rises higher, and more of the GMW outflow is able to exit over the sill (Fig. 4c–d). However, there is still some sill-driven reflux of the GMW outflow in June, and to a lesser extent in July. The subglacial discharge is largest in August, resulting in the shallowest GMW outflow at 0–150 m depth (Fig. 4e). This GMW outflow is able to exit over the sill, with a compensating inflow bringing Disko Bay water into the deep basin (Fig. 4e). The evolution of the melt rate at the glacier front follows the evolution of the plume: a weak plume is associated with a low melt rate and a limited vertical extent of the plume, while in peak summer the plume melt rate reaches 5.1 m d^{-1}, and melt extends up to 40 m depth (Fig. 5). Melt rate is small outside of the plume, resulting in a significantly smaller horizontally averaged melt rate (Fig. 5).

Since the GMW outflow exits over the sill in August, modification in the deep basin, below the 26.9 kg m^{-3} isopycnal is the result of early season entrainment (Figs. 3e and 7). This modification causes the deep basin to be 0.2 °C colder than Disko Bay water at sill depth by peak summer (Figs. 3a–d and Fig. 8). In the surface and intermediate layer, cooling due to the GMW reaches 2 °C in August, compared to the Disko Bay temperature. Overall, glacial modification leads the entire fjord to be almost uniformly 3 °C by August (Fig. 3e). The freshwater flux into the fjord consists of 96% of subglacial discharge, and only 4% out of melt from the glacier front (Fig. 6).

https://doi.org/10.5194/tc-2022-136
Preprint. Discussion started: 8 July 2022
© Author(s) 2022. CC BY 4.0 License.


4.2 Impact of icebergs on the seasonality

Introducing icebergs to the upper 300 m within the fjord leads to significant changes in both water properties and circulation. Since icebergs extend to the warm water layer throughout the year, there is a substantial freshwater flux from the icebergs, also during winter (Fig. 6). This fresh meltwater drives a slight mixing within the intermediate layer and surface during winter (Fig. 4f), which leads to no distinct thermocline, and a notable freshening within the extent of the icebergs (Figs. 3f and 7). The stronger wintertime circulation also increases the frontal melt of the glacier to 4.5 m d^{-1}, compared to 0.7 m d^{-1} *NoIBP*, although the freshwater flux from glacier melt is small compared to iceberg melt (Fig. 6). Spring surface warming in Disko Bay drives iceberg melt in the surface layer, which keeps the surface cold and causes slight freshening (Figs. 3f–j and 8), while also creating outflow in the upper 100 m (Fig. 4e–f). This additional outflow increases the inflow over the sill compared to *NoIBP* (Fig. 4b,g).

As the subglacial discharge season starts in May, the wintertime cooling and freshening caused by icebergs affects the neutral buoyancy depth of the plume: The plume equilibrates 120 m deeper in the water column than in *NoIBP* (Fig 5e). The correspondingly deeper GMW outflow does not exit over the sill, but instead refluxes into the deep basin. These dynamics affect the plume melt rate, which reaches the same peak value at depth, but is limited to below 300 m (Fig. 5a). In June and July when subglacial discharge increases, the plume extends higher in the water column (4h,i). However, the plume remains 50 m deeper, and the GMW outflow close to the glacier is 50–100 m deeper than in *NoIBP*. Furthermore, icebergs melt along the GMW outflow route, due to both the temperature and velocity associated with the outflowing plume (Figs. 6 and S3), leading to a colder intermediate layer than in *NoIBP* (Figs. 3h–i and 8).

In addition to the surface and intermediate layers modification, icebergs modify the deep basin through two separate processes: by entrainment of GMW outflow into the inflowing water to the basin, and by iceberg-modification of inflowing ambient water. While the GMW is also iceberg-modified, we call the incoming ambient water modified by iceberg melt **iceberg-modified ambient water, IMAW**, to separate these two processes of ambient water modification: IMAW has not been in contact with the glacier terminus or the plume, as is the case for GMW. IMAW is present in the deep basin always when there is inflow over the sill and icebergs along the inflow route, whereas GMW will mix into the deep basin when outflow is too deep to exit over the sill. Both processes contribute to cooling and freshening of the deep basin (Fig. 3g–j and 8), which is also reflected in a slight decrease of the plume melt rate at depth (Fig. 5b–c).

The plume reaches higher up the watercolumn in August — still 50 m deeper than in *NoIBP* — and the GMW outflow takes place at 100 m depth, with some slight entrainment into the inflowing waters (Fig. 4h). The fjord has a cold surface, cool intermediate layer and slightly cooled deep basin water (Fig. 3j). Meanwhile, relatively warmer plume water reaching the icebergs drives iceberg melt, with a peak melt value of 1540 m^3 s^{-1} (Fig. 6). The increase in iceberg melt from July to August is primarily due to an increase in drift-induced melt, as temperature does not increase (Figs. 3i–j and S3). The additional outflow due to iceberg melt is compensated by a stronger inflow over the sill, increasing the volumetric flow rate over the sill by 50%, from $1 * 10^5$ m^3 s^{-1} in *NoIBP* to $1.5 * 10^5$ m^3 s^{-1} in *IBP*. The iceberg-melt driven circulation directs more of the inflowing water towards the base of the icebergs, rather than deeper into the basin (Fig. 4j). The modelled August GMW

https://doi.org/10.5194/tc-2022-136
Preprint. Discussion started: 8 July 2022
© Author(s) 2022. CC BY 4.0 License.


outflow takes place within the 26.3 kg m^{-3} and 26.5 kg m^{-3} density layers, while the surface above 26.3 kg m^{-3} is dominated by iceberg melt (Fig. 7 and Fig. 3j). The inflow region is located below approximately 200 m depth and isopycnal 26.5 kg m^{-3}, and the inflow can be further divided into three vertical layers: 26.5–26.7 kg m^{-3} is the rapid inflow region at the base of the icebergs, containing IMAW mixed with entrained GMW outflow water, 26.7–26.8 kg m^{-3} contains only IMAW, and water below 26.8 kg m^{-3} contains IMAW mixed with early season GMW.

To sum up, icebergs modify the fjord properties and circulation in three main ways: Firstly, by cooling and freshening the surface and intermediate layers through iceberg melt; Secondly, by causing the plume and GMW outflow to be deeper; Thirdly, by modifying the deep basin water through iceberg modification of inflowing ambient water (IMAW), and entrainment of GMW into the inflow into the deep basin. These changes impact the melt rate by reducing the melt rate at depth, due to the cooling of the deep basin, and by the limited vertical extent due to the plume being deeper (Fig. 5). Thus, iceberg-modification of the fjord will cause less melt of the glacier, and the melt will be limited to the deep part of the glacier front (Fig. 11).

4.3 Comparison to observations

The observed temperature in the fjord shows a cold and fresh surface layer, cooled intermediate layer water and a slightly modified deep basin (Figs. 3m and 8) — which is consistent with the results of experiment *IBP* (Fig. 3j). In the observations, the GMW outflow is mostly located between isopycnals 26.3 kg m^{-3} and 26.9 kg m^{-3}, corresponding to a relatively narrow depth range of approximately 100–200 m (Figs. 3m and 7). Even though the density of the GMW outflow is different in the observations and in *IBP*, the deepest extent of a significant contribution of GMW outflow is approximately 200 m for both in the mid-fjord location (Fig. 8). Below 26.9 kg m^{-3}, the observed deep basin is dominated by melt, following the melt line almost perfectly with negligible contribution of surface runoff, except for the profile directly next to the glacier (Fig. 7). We interpret this to indicate a large contribution of IMAW rather than GMW. IMAW is, by definition, formed along the inflow route into the fjord. Thus, a layer in the fjord filled with purely IMAW would be a layer of inflow towards the glacier. This suggests that 26.9 kg m^{-3} could distinguish between inflow and outflow in the fjord.

4.4 The relative impact of plume width and iceberg distribution on fjord properties

We run three different plumes and three different iceberg distributions from winter to peak summer in order to investigate the sensitivity of our results to plume width and iceberg distribution (Table 1). Comparisons of temperature, circulation and melt rate demonstrate the separate contributions of the plume and iceberg distribution, and also the separate impact GMW and IMAW have on the deep basin properties (Figs. 9 and 10). Plume width is the primary controlling factor of the vertical extent of the plume. Changes in the depth of the GMW outflow determine the circulation of the fjord, which are reflected in the fjord temperature and maximum melt rate of the plume. Decreasing plume width creates a more concentrated plume that entrains less deep basin water into the plume, and thus rises higher in the water column, transporting heat efficiently up (Fig. 9). This concentrated plume leads to a higher and more concentrated outflow of GMW, which is less prone to entrain into inflowing water at the sill, leading to a less modified deep basin (Fig. 9c,f,i). For the wide plume, on the other hand, deep basin water entrainment into the plume is more efficient, causing the plume to remain deep, leading to entrainment of GMW even during

https://doi.org/10.5194/tc-2022-136
Preprint. Discussion started: 8 July 2022
© Author(s) 2022. CC BY 4.0 License.

The Cryosphere
Discussions
Open Access
EGU

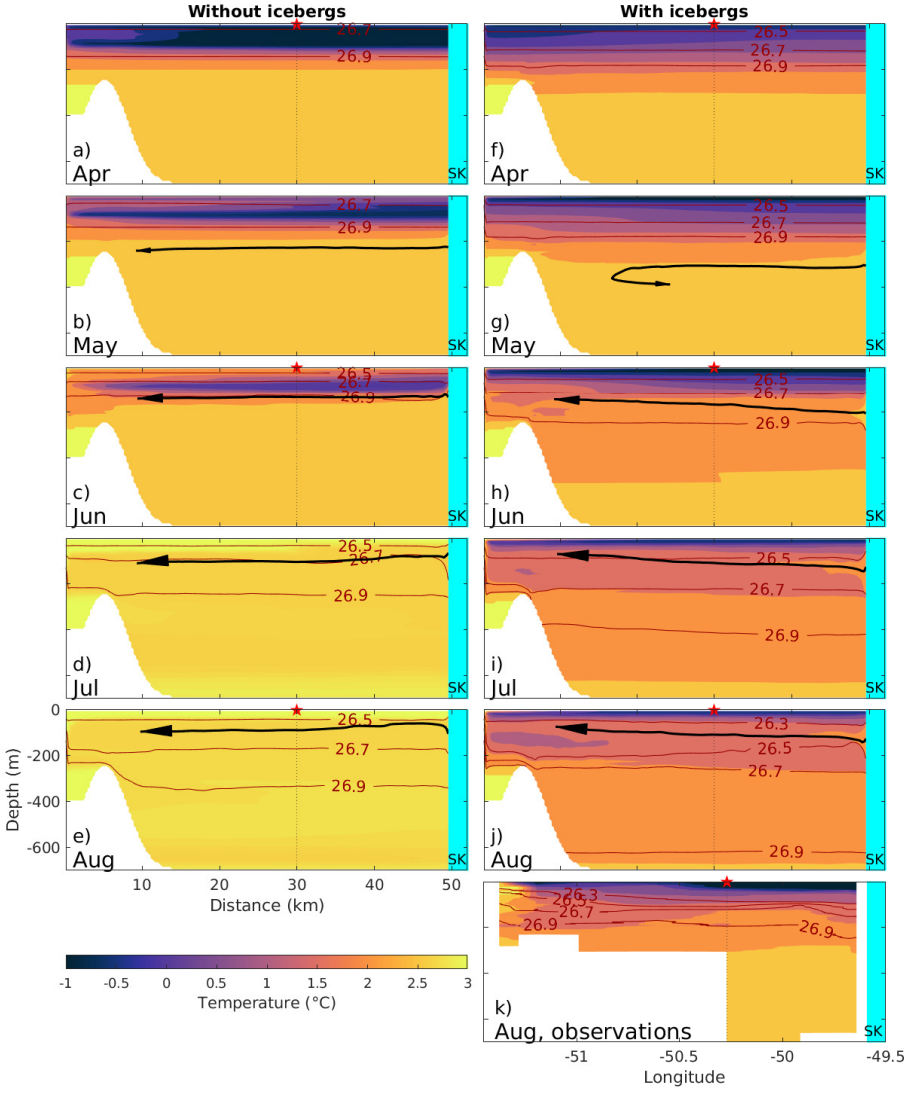

Figure 3. Along-fjord temperature sections for Ilulissat Icefjord with (f–j), *IBP*) and without icebergs (a–e), *NoIBP*), from onset of spring (April) to peak summer (August), as a snapshot at the end of each month. k) observed temperature section from XCTD data in August 2014 (Beaird et al., 2017), XCTD locations are marked in Fig 1. Red contours mark the isopycnals of 26.3 kg m^{-3}, 26.5 kg m^{-3}, 26.7 kg m^{-3} and 26.9 kg m^{-3}. Black arrows indicate the centerline of the outflow of glacially modified water from the plume (See also Fig. 4).

https://doi.org/10.5194/tc-2022-136
Preprint. Discussion started: 8 July 2022
© Author(s) 2022. CC BY 4.0 License.

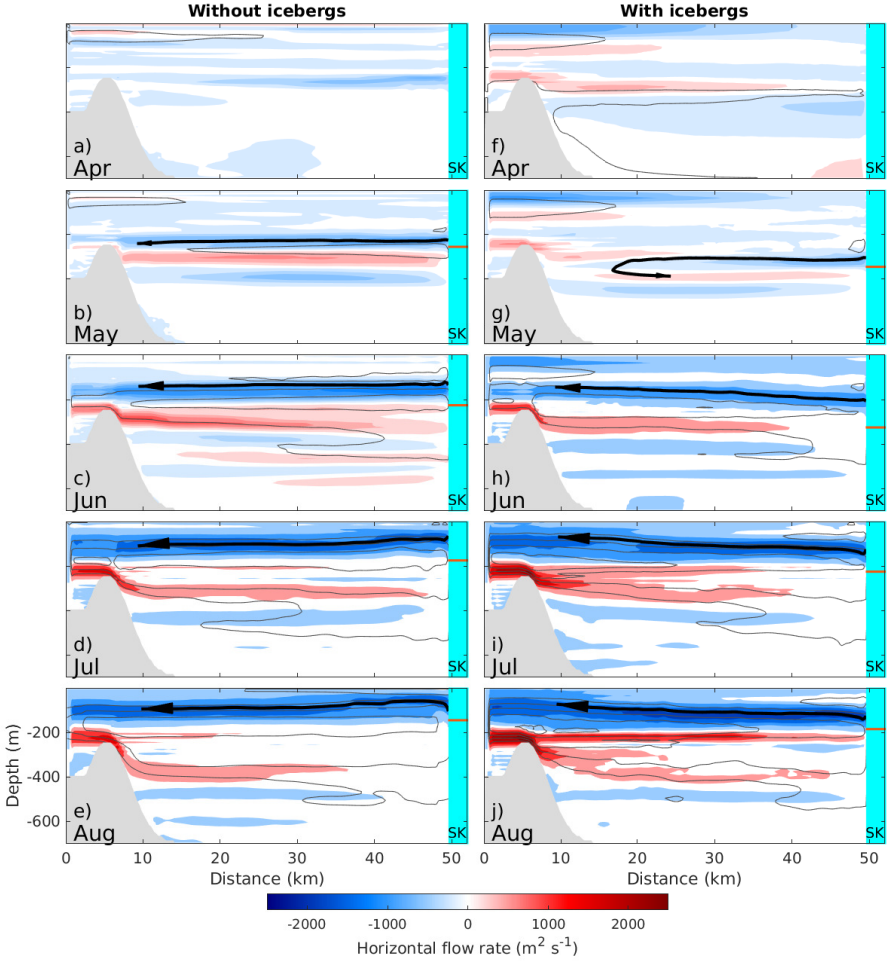

Figure 4. Snapshots of horizontal flow rate along the fjord from the start of the subglacial discharge season in May to peak summer in August, a–d) without icebergs (NoIBP), and e–h) including icebergs (IBP). Black arrow indicates the centerline of the GMW outflow from the plume, and grey contours streamlines of the horizontal flow rate at 0.02 m^3 d^{-1} intervals. Red horizontal line marked on the pale blue glacier front indicates the neutral buoyancy depth of the plume.

https://doi.org/10.5194/tc-2022-136
Preprint. Discussion started: 8 July 2022
© Author(s) 2022. CC BY 4.0 License.

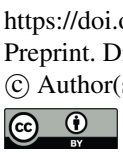

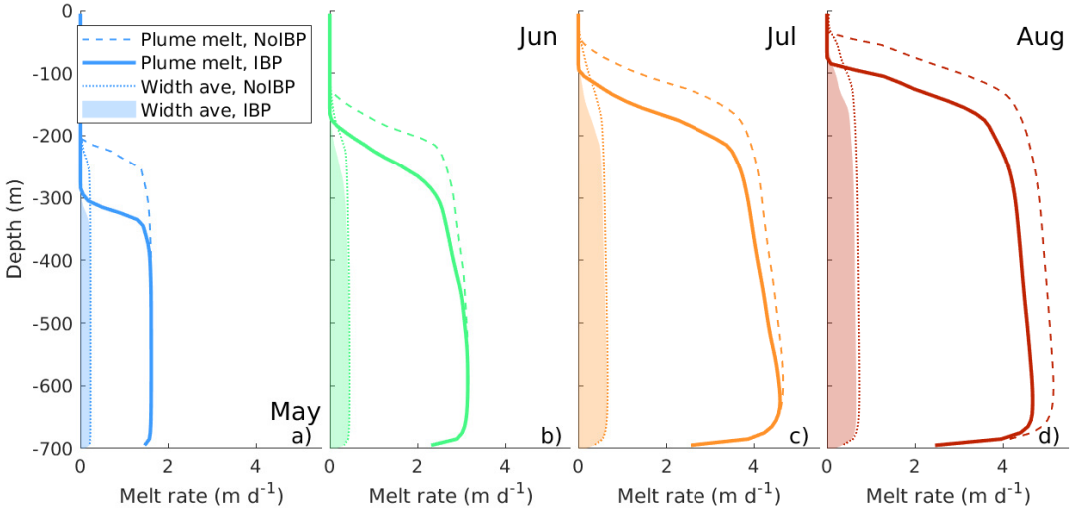

Figure 5. Seasonality of frontal melt of the glacier from May to August as both plume melt rate for *NoIBP* (dashed line), and *IBP* (solid line), and also width-averaged frontal melt rate for both *NoIBP* (dotted line) and *IBP* (shaded area).

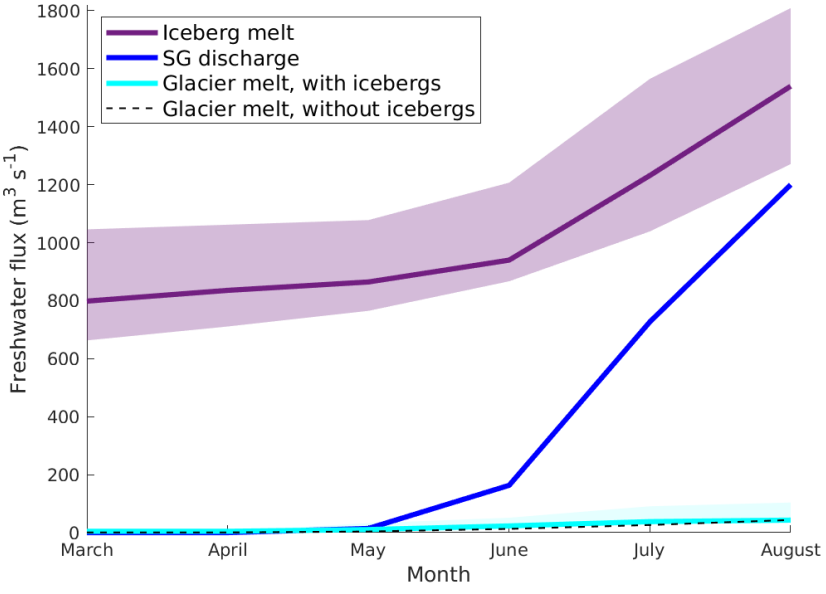

Figure 6. Modelled seasonality of the freshwater volume flux into Ilulissat Icefjord from different sources: icebergs (*IBP*, purple), subglacial discharge forcing (blue line) and glacier melt for *NoIBP* (dashed black line) and *IBP* (pale blue). Shadings indicate the range covered by the sensitivity experiments (see Table 1 and Sect. 4.4).

https://doi.org/10.5194/tc-2022-136
Preprint. Discussion started: 8 July 2022
© Author(s) 2022. CC BY 4.0 License.

The Cryosphere
Discussions
Open Access
EGU

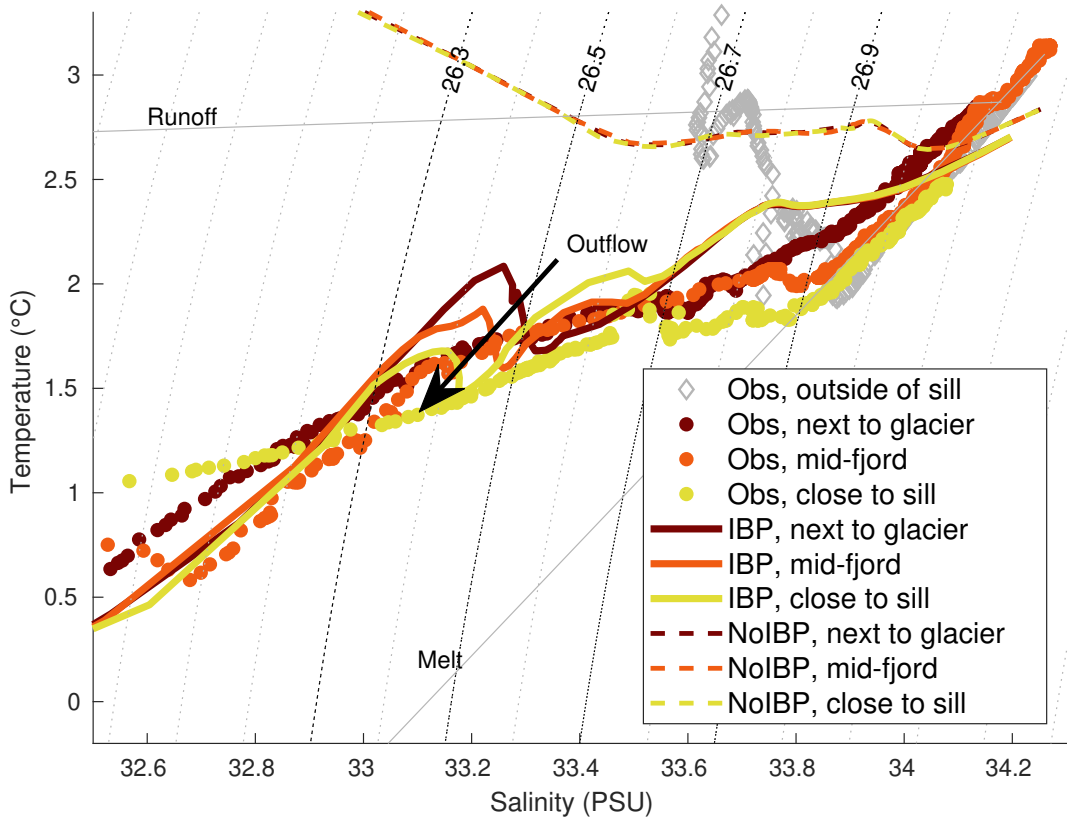

Figure 7. August potential temperature versus salinity next to the glacier (brown), mid-fjord (orange) and close to the sill (yellow), for observations (circles) (Beaird et al., 2017), *IBP* (solid lines) and *NoIBP* (dashed lines), with runoff and melt lines (grey lines) and isopycnals (dotted grey lines). Grey dotted contours indicate isopycnals at 0.1 kg m^{-1} intervals, with 26.3 kg m^{-1}, 26.5 kg m^{-1}, 26.7 kg m^{-1} and 26.9 kg m^{-1} indicated in black (Also plotted in Fig. 3).

peak summer, and significant modification of the deep basin properties (Fig. 9a,d,g). While the peak plume melt rate for the wide plume is less than half that of the narrow plume, the horizontally averaged melt rate is significantly higher (Fig. 10).

Iceberg depth impacts the properties of the intermediate layer and the deep basin, as the extent of the cooling and freshening increases with increasing iceberg depth (Fig. 9). These changes are a result of the combined effect of increased contribution of IMAW with iceberg depth, and the entrainment of increasingly iceberg-modified GMW. Icebergs depress the neutral buoyancy depth of the plume, the more the wider the plume, as more iceberg-modified ambient water is entrained into the plume (Fig. 10a, grey shaded areas compared to lines). Iceberg distributions *IB* and *IB400* have similar number of icebergs within the top 300 m (Fig. 10c), and thus the differences in the neutral buoyancy depth are small between these two iceberg distributions. *IB200*, however, has approximately twice as many icebergs within the top 200 m as the other two distributions, leading to the neutral buoyancy depth being depressed by 20 m more than for the default and narrow plumes. On the other hand, *IB200WP* has less

https://doi.org/10.5194/tc-2022-136
Preprint. Discussion started: 8 July 2022
© Author(s) 2022. CC BY 4.0 License.

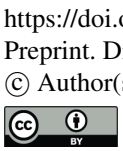

The Cryosphere
Discussions
Open Access
EGU

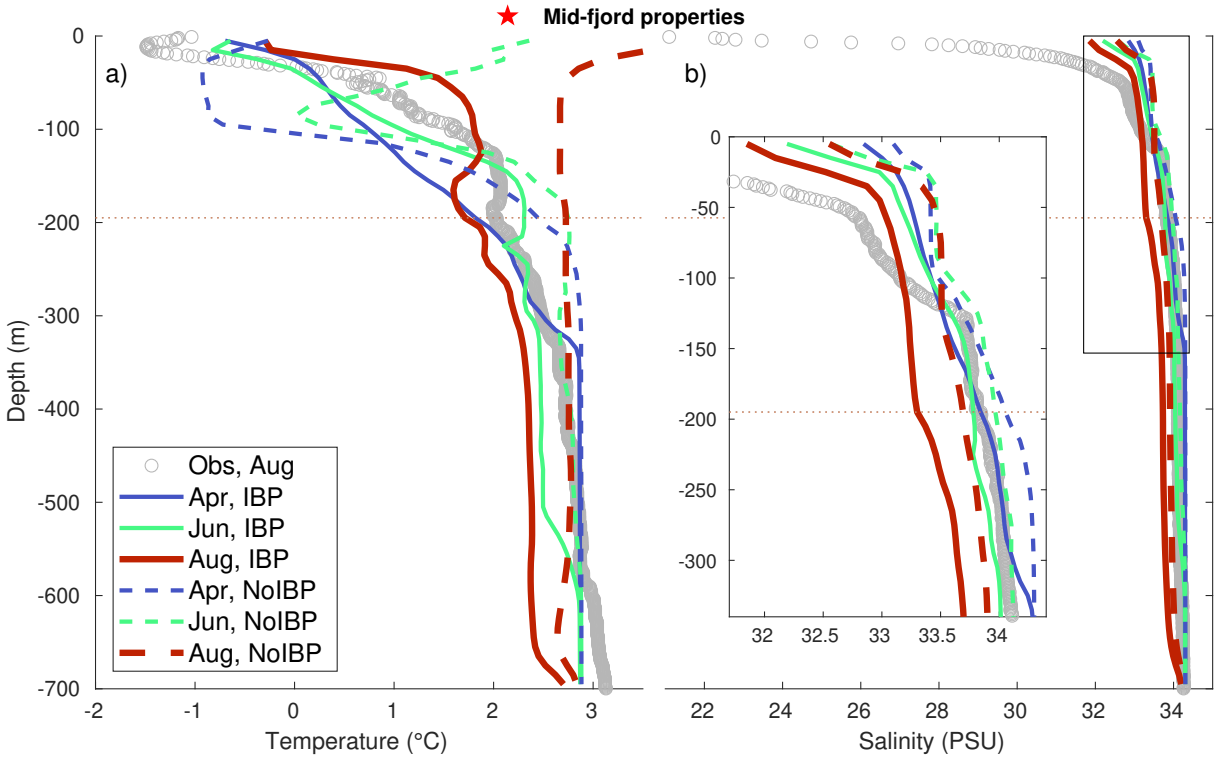

Figure 8. Mid-fjord temperature and salinity profiles for April, June and August for both *IBP* (solid lines), *NoIBP* (dashed lines). Grey circles indicate the XCTD profiles in August 2014 (Beaird et al., 2017). The dotted horizontal line marks 195 m depth, which coincides in *IBP* with isopycnal 26.5 kg m^{-3} and the inflow/outflow border in August, and in the observations with isopycnal 26.9 kg m^{-3}. Mid-fjord location is indicated with red star and vertical dotted lines in Fig. 3 and in Fig. 1.

iceberg modification of the plume than the other two distributions, since the neutral buoyancy depth is below the maximum iceberg extent ('WP' lines in Fig. 10a). Overall, this indicates that the number of icebergs extending down to the expected neutral buoyancy depth imposes a stronger control than the maximum iceberg depth. Iceberg-induced deep basin cooling decreases the maximum plume melt rate at depth, but this effect is small (Fig. 10a).

The sensitivity experiments demonstrate the separate contributions of IMAW and GMW, as IMAW contribution in the deep basin increases with iceberg depth, and GWM contribution decreases when decreasing the plume width. *IB400NP* has a narrow plume, causing GMW to exit right below the surface layer, leaving the deep basin unmodified by the GMW, except for a small early-season contribution. However, since *IB400NP* has deep icebergs, the resulting deep basin has a significant IMAW contribution (Fig. 9i). Conversely, *IB200NP* has icebergs shallower than the sill depth, leading to no IMAW and very little early-season GMW in the deep basin (Fig. 9c). *IB200WP*, meanwhile, has similarly negligible IMAW contribution and iceberg-modification of the entraining GMW (Fig. 9a), however, the overall entrainment of the GMW is significant due to the wide plume, leading to significant modification of the deep basin with little contribution from the icebergs. The significance

https://doi.org/10.5194/tc-2022-136
Preprint. Discussion started: 8 July 2022
© Author(s) 2022. CC BY 4.0 License.

260 of early-season processes to the summer temperature profile is clearly demonstrated by *IBNP*, where the early-season iceberg-modified water is located at 400–600 m depth, below less modified water inflowing during peak summer (Fig. 9f). These results show that — while the plume is a determining factor for the circulation in the fjord — increasing iceberg depth increases modification in the deep basin.

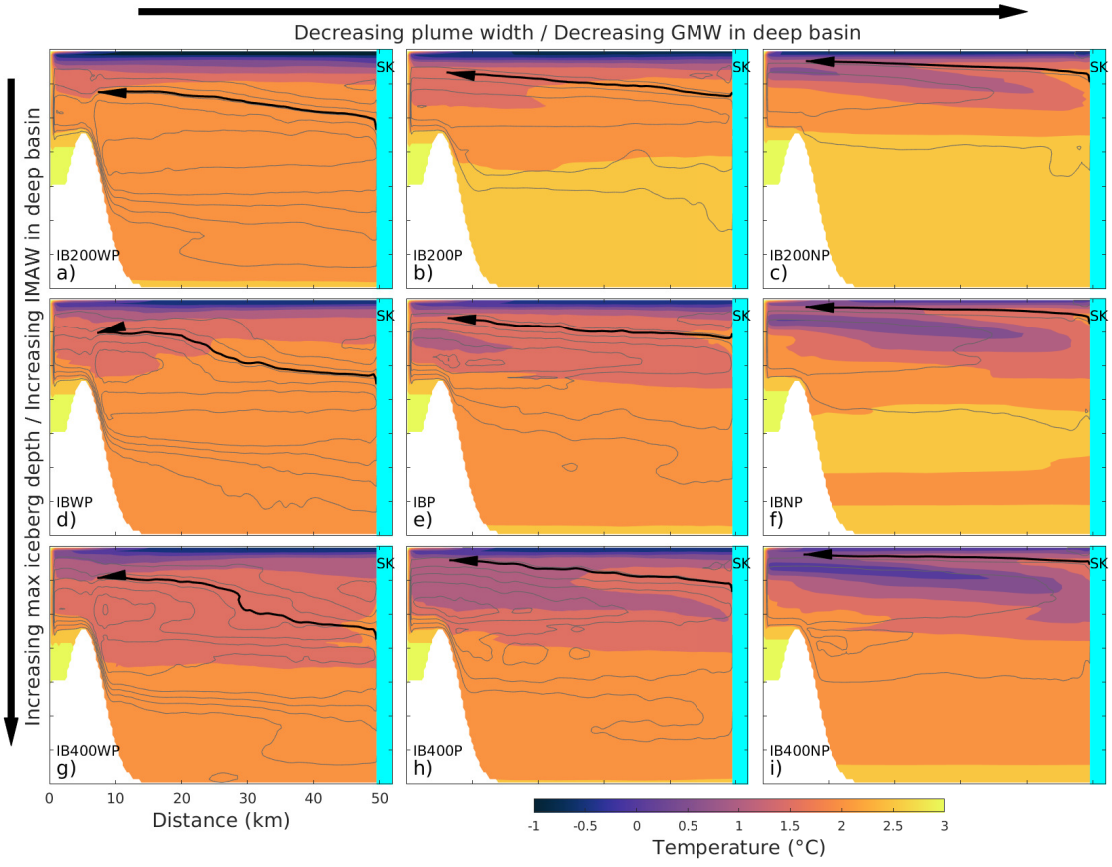

Figure 9. August along-fjord sections of horizontally averaged temperature for all sensitivity experiments with three different plumes (columns), and three different iceberg distributions (rows). See Table 1 for experiment naming. Black arrow indicates the centerline of the GMW outflow from the plume, and grey contours a snapshot of streamlines of the horizontal flow rate at 0.02 m^3 d^{-1} intervals.

https://doi.org/10.5194/tc-2022-136
Preprint. Discussion started: 8 July 2022
© Author(s) 2022. CC BY 4.0 License.

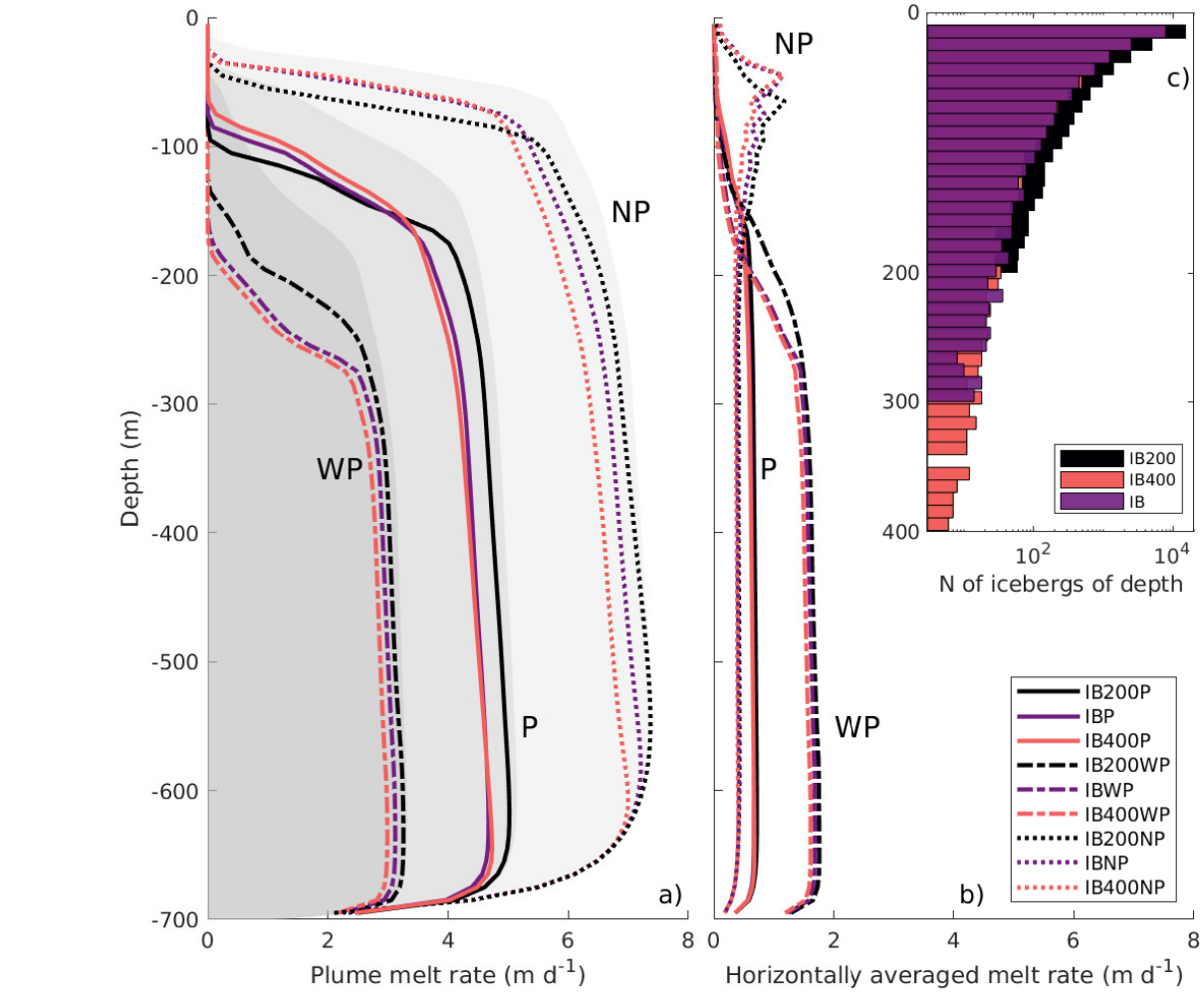

Figure 10. August vertical melt rate profiles for a) plume melt and b) horizontally averaged frontal melt for the nine iceberg experiments with three different iceberg distributions (colors, see panel c) for color labels), and wide (WP), default (P) and narrow plumes (NP) (semi-dashed, solid, and dotted lines respectively). See Table 1 for experiment naming. The three different grey shadings in panel a) indicate the vertical melt rate profile of each of the three plumes without icebergs. c) shows the number of icebergs extending to a certain depth at 10 m intervals in the three used iceberg distributions.

https://doi.org/10.5194/tc-2022-136
Preprint. Discussion started: 8 July 2022
© Author(s) 2022. CC BY 4.0 License.


5 Discussion

5.1 Iceberg modification in Ilulissat Icefjord

Our results show that icebergs must be included in order reproduce the water column properties of Ilulissat Icefjord. Icebergs cool and freshen the entire water column of the fjord, most intensely in the top 50 m, which hosts a large number of small icebergs. Our simulation including icebergs matches well with the observed temperature profile in Ilulissat Icefjord in August 2014 (Fig. 3j,m), which is typical for Ilulissat Icefjord in peak summer (Gladish et al., 2015; Fenty, I. et al., 2016; Beaird et al., 2017; Mojica et al., 2021). We find that iceberg melt is the main source of cooling in the surface and intermediate layers of the fjord, while the combined effect of subglacial discharge and frontal melt of the glacier only account for approximately 25% of the simulated cooling (Fig. 8a); The iceberg-induced cooling and freshening reaches up to 4 °C and 0.7 PSU in peak summer (Fig. 8). This matches well with the cooling and freshening of 5 °C and 0.7 PSU simulated for Sermilink Fjord in southeastern Greenland by Davison et al. (2020) with a similar iceberg distribution. Comparison of *IBP* and *NoIBP* to observations in TS-space further highlights the contribution of iceberg melt (Fig. 7). The small contribution of subglacial discharge and direct glacier melt is supported by findings from other West Greenland fjords, which show that the majority of glacial modification takes place along the fjord — through, for example, iceberg melt — while direct melt from the glacier terminus and subglacial discharge are a small contributor (Mortensen et al., 2020; Muilwijk et al., 2021). Our model slightly underestimates the surface cooling and freshening, which we assume to be due to the exclusion of runoff to the surface of the fjord (Mernild et al., 2015), or possibly due to underestimated contribution from small icebergs by the power law size distribution (Rezvanbehbahani et al., 2020).

We find that the iceberg-induced cooling and freshening in the intermediate layer depresses the neutral buoyancy depth of the plume and the outflow route of the GMW (Illustrated in Fig. 11). This is supported by Beaird et al. (2017) who find the water above 250 m close to the glacier to be anomalously cold compared to what is predicted by plume theory, indicating a depressed plume. They speculate that this mismatch is due to the impact of icebergs, which our model results confirm. Previous estimates of the neutral buoyancy depth of the plume of Sermeq Kujalleq in peak summer range from 350 m depth to the surface (Jenkins, 2011; Gladish et al., 2015; Carroll et al., 2016), depending on the subglacial discharge flux, ambient water properties and ice front shape. Truffer and Motyka (2016) briefly speculate on the possibility that the ice melange could mechanically prevent the plume to reach the surface in the Ilulissat Icefjord. However, since the melange is not rigid during peak summer (Joughin et al., 2020), we argue that the plume is deep due to the iceberg induced stratification, rather than a mechanical effect. A similar phenomenon but at much smaller scale was observed in the nearby Saqqarlep fjord, where extreme melt caused surface freshening and thus prevented the plume from reaching the surface, as it normally does in this location (De Andrés et al., 2020).

Davison et al. (2022) study the impact of icebergs on plume melt in an idealized fjord setup, but do not find significant changes in plume temperature and melt rate. They study a 500 m fjord with a single point-source plume, which has limited entrainment of ambient water into the plume, and is thus relatively unaffected by iceberg-modification of the fjord water (Fig. 9 in (Davison et al., 2022)). Their plume reaches the surface in all their different iceberg distributions, but since they do

https://doi.org/10.5194/tc-2022-136
Preprint. Discussion started: 8 July 2022
© Author(s) 2022. CC BY 4.0 License.

not discuss stratification or buoyancy, it is not clear if the neutral buoyancy depth changes in their different iceberg distributions. However, since Jackson et al. (2017) suggest that wide plumes match better with observations, and observations by Beaird et al. (2017) support our model results, we conclude that a plume with a width on the hundred-meter-scale is more realistic.

The depressed plume leads to enhanced basin water modification due to increased entrainment of GMW outflow into inflowing Disko Bay water, as not all outflow is able to exit over the sill (Fig. 11b). However, icebergs also modify directly the inflowing ambient water from Disko Bay, creating iceberg-modified ambient water (IMAW) that has not had any contact with the glacier front or the plume. Both GMW and IMAW are typically present in a high-silled fjord with a marine terminating glacier, such as Ilulissat Icefjord, however, their origin are different. Thus, even if the GMW outflow is able to completely exit the fjord, the deep basin water will still be modified by IMAW, as long as there are icebergs present along the inflow route. Modification of the deep basin of Ilulissat Icefjord is supported by Beaird et al. (2017), who find the fjord to be glacially modified to at least 600 m depth. This interpretation is different from Gladish et al. (2015), who describe the basin to be filled with Disko Bay water at sill depth, with no significant glacial modification. Since their model lacks both icebergs and seasonal considerations, all GMW will exit the fjord, leading to no modification in the deep basin. Our results highlight the importance of including both icebergs and seasonal variations of subglacial discharge. Davison et al. (2020) find that icebergs increase heat transfer towards the glacier due to iceberg-melt-driven estuarine circulation in Sermilink Fjord and for an idealized fjord without a sill. However, Davison et al. (2022) do observe that when icebergs extend below sill depth, the deep basin is cooled, as it does in our model. Our analysis explains the dynamics of GMW depression and IMAW formation at the high sill that leads to this iceberg-iduced deep basin modification. Hager et al. (2022) also discover a similar mixing of GMW outflow down into the deep basin in a high silled glacial fjord in LeConte Bay in Alaska. Our results together with Davison et al. (2022) and Hager et al. (2022) show that high sills in glacial fjords are significant not only as barriers preventing warm ambient water inflow, but contribute to deep basin water modification.

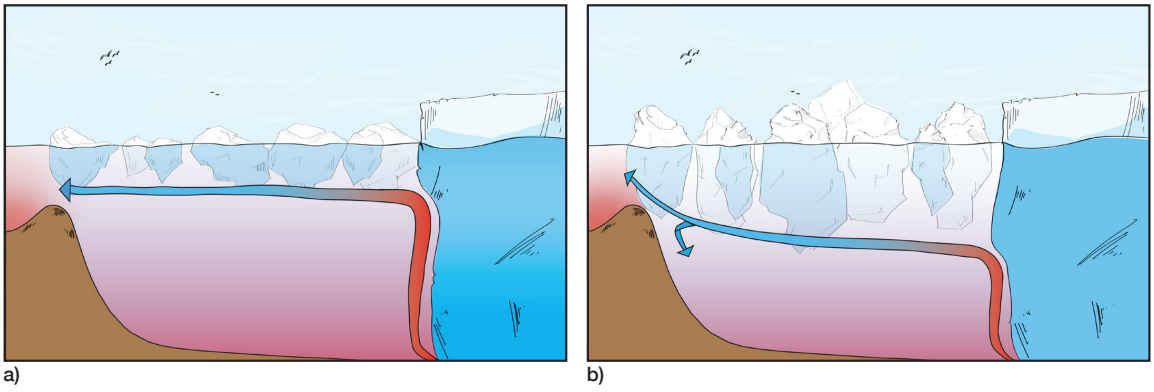

Figure 11. Illustration of iceberg modification of the plume and GMW outflow. Icebergs depress the neutral buoyancy depth of the plume and the subsequent GMW outflow. The GMW outflow gets further modified by icebergs, and mixes partially back into the fjord, when reaching a high sill.

https://doi.org/10.5194/tc-2022-136
Preprint. Discussion started: 8 July 2022
© Author(s) 2022. CC BY 4.0 License.


5.2 Subglacial dischare as a driver of seasonality

In our model, as in previous studies of high-silled fjords (Gladish et al., 2015; Carroll et al., 2017), the plume drives the circulation in the fjord. We find subglacial discharge to be the primary driver of seasonality of the circulation, as the high sill prevents the outflow of a weak early-season plume, leading to basin water modification. Hager et al. (2022) discover a similar strong dynamics in LeConte Bay, where seasonal changes in subglacial discharge drive significantly different circulation patterns. We find that seasonal surface warming in Disko Bay has little impact in the fjord when icebergs are included. Subglacial discharge is also the driver of seasonality in the freshwater flux from icebergs in our model, which we estimate to be 660–1050 $m^3\ s^{-1}$ in winter and 1270–1810 $m^3\ s^{-1}$ in peak summer. This is in line with previous satellite-derived estimates of 678–1346 $m^3\ s^{-1}$ and 1300–1700 $m^3\ s^{-1}$ for Sermeq Kujalleq in peak summer (Enderlin et al., 2016; Mankoff et al., 2020). Wintertime freshwater flux is estimated to be several hundreds of $m^3\ s^{-1}$ (Enderlin et al., 2016). Moon et al. (2018) estimate the peak iceberg freshwater flux for Sermilink Fjord to take place later in the season, September to November, since the volume of icebergs in the fjord accumulates throughout the calving season. We do not consider variability of the iceberg distribution during the experiments; however, our sensitivity experiments show that the increase in iceberg melt due to the plume is larger than the variability of the freshwater flux due to the iceberg distribution (Fig. 6).

Subglacial discharge drives the seasonality of the glacier melt rate, both of the maximum melt rate and of the vertical reach of the plume (Fig. 5). Observational studies of Sermeq Kujalleq indicate that there is a link between iceberg melange and seasonal changes in calving rate, as a reduction of calving during winter and the growth of rigid melange seem to correlate (Joughin et al., 2008; Cassotto et al., 2015; Joughin et al., 2020). Melt rate is connected to calving through either the calving-multiplier effect or a destabilizing influence, but the exact processes are elusive and location dependent (O'Leary and Christoffersen, 2013; Rignot et al., 2015; Benn and Åström, 2018; Cowton et al., 2019; Cook et al., 2021; Slater et al., 2021). Our results show that melt is localized at depth, particularly for the early season. Melt localized at depth promotes undercutting, which is the determining factor for calving style (Benn and Åström, 2018; Slater et al., 2021). Currently, bottom-out rotation is preferential for Sermeq Kujalleq (Amundson et al., 2010; Cassotto et al., 2019), suggesting that undercutting driven by melt is the main driver of calving. Thus, we speculate that as subglacial discharge drives seasonality in melt rate, it will also drive seasonality of undercutting and thus calving of this glacier. Our results are in line with previous studies, indicating that subglacial discharge has a strong control of the melt rate, both through discharge volume (Jenkins, 2011; Truffer and Motyka, 2016), but also through the suglacial-drainage-system properties that ultimately control the plume height (Khazendar et al., 2019; Straneo et al., 2019; Cook et al., 2021).

The connection between iceberg melange and the suppression of calving is sometimes attributed to mechanical support by a rigid melange that prevents calving (Joughin et al., 2008; Burton et al., 2018; Joughin et al., 2020). However, mechanical support disappears once the rigidity is lost, as the non-rigid melange is a granular material, able to compact and relax under calving events (Peters et al., 2015). The presence of reliably rigid melange in Ilulissat Icefjord varies inter-annually, and it has been present only sporadically in the previous decade (Cassotto et al., 2015; Joughin et al., 2020), and thus does not give a comprehensive explanation to the link between melange and calving. Since our results show that icebergs limit melt to the

https://doi.org/10.5194/tc-2022-136
Preprint. Discussion started: 8 July 2022
© Author(s) 2022. CC BY 4.0 License.


deep part of the glacier front, we hypothesize that icebergs moderate calving by strengthening undercutting. Furthermore, our results indicate that the plume significantly increases currents within the iceberg melange (Fig. S3), likely inhibiting rigid melange formation. Thus, we see the seasonal growth of rigid melange as a consequence of decreased melting and calving due to a weakening plume. Mernild et al. (2015) find autumn cooling in the deep basin of Ilulissat Icefjord, which could be a consequence of increased entrainment and iceberg modification as the plume weakens, similarly as for the weak spring plume in our model (Fig. 4g). In this case cooling due to increased entrainment and modification would further reduce the melt rate of the glacier, amplifying the winter suppression of melt.

Iceberg control over the neutral buoyancy depth of the plume provides a mechanism for the iceberg melange to influence melt, even during peak summer discharge when the melange is not rigid. In the absence of a physical understanding of calving it is difficult to make quantitative estimates of how a certain deepening of the neutral buoyancy depth of the plume would impact calving, and we see this as a key point of further study. Further study is also needed on iceberg-plume-GMW dynamics, and on how this dynamics will evolve in a warming climate. Much will depend on how the subglacial drainage system will react to longer and more intense melt seasons. Increased calving has the potential to strengthen the iceberg-induced modification in the Ilulissat Icefjord: As Sermeq Kujalleq is predicted to retreat into even deeper geometry (Bondzio et al., 2017). Therefore, maximum iceberg depth and thus iceberg modification in the deep basin can be expected to increase.

5.3 Model uncertainties

One of the key features of the IceBerg package is that the icebergs do not move or change volume when melting, and we choose not to edit the distribution manually during experiments. While the iceberg cover of the Ilulissat Icefjord is a relatively constant feature, due to the large calving flux of the glacier, observations indicate some annual variability (Cassotto et al., 2015; Enderlin et al., 2016; Joughin et al., 2020). We expect the range of iceberg distributions applied in the sensitivity experiments to span the natural variability, and also along-fjord variations of the iceberg distribution in the Ilulissat Icefjord (Sec. 4.4). We do not expect temporary reductions in the iceberg cover to impact the hydrography of the fjord to a large degree. Observations of summer surface conditions in Ilulissat Icefjord in 2000–2011 show consistently an iceberg-dominated surface at melting point (Cassotto et al., 2015), which makes us assume that any deviations are short in duration.

Our modelled iceberg distribution produces slightly cooler and fresher deep basin than what is observed (Fig. 3f–m), which seems to be a combination of slightly different properties of the deepest water in the basin, and an overestimated contribution of subglacial discharge within the deep basin (Fig. 7). In the model, GMW in the basin is largely a product of early season mixing at the sill, which in reality could be reduced due to shallow or sparse iceberg distribution at the sill early in the season. The good correspondence between the observations and sensitivity experiment *IB200P* (Figs. 3m and 9b) indicates that icebergs could have been shallower in 2014 than modelled. (Enderlin et al., 2016) shows that in June 2014 icebergs in Ilulissat Icefjord were indeed relatively shallow, further supporting this interpretation. We keep the properties of Disko Bay water at sill depth constant for simplicity, but variability at the sill could cause dense water inflows that contribute to the deep basin properties. Also, we assume that each phase of the seasonal evolution of the subglacial discharge is equal — 30 days of duration — which

https://doi.org/10.5194/tc-2022-136
Preprint. Discussion started: 8 July 2022
© Author(s) 2022. CC BY 4.0 License.


could potentially overestimate the early season contribution. The seasonality of subglacial discharge is likely to vary greatly both intra and interannually (Cook et al., 2021).

The IceBerg package implements freshening due to iceberg melt by applying a negative salinity anomaly. In reality we would expect the icebergs to be a source of freshwater input to the fjord (Mernild et al., 2015; Enderlin et al., 2016; Moon et al., 2018). The negative salinity approach forces the modelled inflow and outflow of the iceberg-melt driven circulation to be equal in volume, leading to a 50% increase in the volume flux over the sill, when including icebergs (Fig. 4d,h). This creates a rapid inflow at the base of the icebergs, increasing drift-induced melt. More observations are needed to analyse if the negative salinity approach overestimates the inflow over the sill, which we would expect to be smaller than outflow if icebergs are considered as a source of freshwater. We do not include tides or rotational effects, since their impacta are small in our high-silled setup (Carroll et al., 2017). However, both of these effects should be considered in a bathymetrically accurate study of Ilulissat Icefjord, since they could potentially impact the mixing at the sill: rotation could redistribute the GMW outflow laterally, while tides would increase mixing at the sill (Carroll et al., 2017), potentially increasing iceberg melt at the sill.

Icebergs are represented by cell-averaged temperature and salinity forcings in the IceBerg package(Davison et al., 2020), and thus we do not consider icebergs as obstacles for flow. However, individual icebergs alter the circulation by creating a complicated flow network, which slows down the near-surface current (Hughes). This mechanical effect of the icebergs would also cause depression of the GMW outflow, complementing our modelled ~~the~~ stratification-driven depression. Furthermore, we do not consider variations to the melt rate parameterizations due to different flow regimes, as described in (Fitzmaurice et al., 2018), which could be a further development point for the IceBerg package. For simplicity, we choose to use standard values of the turbulent transfer coefficients for both heat and salt transfer both for the glacier and for the icebergs (Table. S1). Jackson et al. (2020) suggest new, higher values for the turbulence parameters, and (Davison et al., 2020) tests the possibility of varying these parameters for icebeg melt. Given that their study shows that increased values of turbulent transfer enhance the impacts of icebergs, we consider the standard values to be a conservative estimate. The turbulence parameters at the glacier front have negligible impact to the results as frontal melt is such a small contributor in the fjord (Fig. 6).

6 Conclusions

We find that icebergs are the key factor modifying the water mass properties of the Ilulissat Icefjord, and that omitting icebergs can lead to misleading interpretations of both water mass properties and the glacier's response to external forcing. Icebergs impact Ilulissat Icefjord in three main ways: First, icebergs cool and freshen the water column within their vertical extent; Second, icebergs limit the vertical reach of the plume, by deepening the neutral buoyancy depth and the outflow route of glacially modified water; Third, icebergs modify the deep basin, below their vertical extent, due to both increased mixing of glacially modified outflow into the fjord at the high sill, and iceberg modification of the incoming ambient water from Disko Bay. Entrainment is particularly important early in the season, when subglacial discharge is weak. The seasonal evolution of the subglacial discharge flux is the primary control of the seasonality of the plume and frontal melt rate, which further supports the idea of the plume as a driver of seasonality in undercutting and thus calving. During peak summer discharge, icebergs

https://doi.org/10.5194/tc-2022-136
Preprint. Discussion started: 8 July 2022
© Author(s) 2022. CC BY 4.0 License.


depress the plume and thus limit glacier melt to the deep part of the glacier front. We postulate that the impact of icebergs on the neutral buoyancy depth of the plume is a key mechanism moderating glacier calving in Ilulissat Icefjord, and provides a comprehensive link between iceberg melange and glacier calving.

Code availability. MITgcm is freely available at https://github.com/MITgcm/MITgcm/archive/master.zip and https://doi.org/10.5281/zenodo.4968496 (Marshall et al., 1997). The IcePlume module is available from Tom Cowton on request. The IceBerg module is available at https://doi.org/10.5281/zenodo.3979647 (Davison et al., 2020).

Data availability. The model domain, boundary conditions and output are available from the corresponding author on request.

Author contributions. KK and KHN conceived the study. KK designed and conducted the simulations and analysis, and wrote the original manuscript. FS and KHN supported the interpretation of the model results and contributed to the preparation of the manuscript.

Competing interests. KHN is a member of the editorial board of The Cryosphere. The authors declare that no other conflicts of interest are present.

Acknowledgements. KK and KHN were supported by the European Research Council under the European Community's Seventh Framework Program (FP7/2007-2013) / ERC grant agreement 610055 as part of the ice2ice project. KHN is also supported by the ClimateNarratives NRC grant(324520). FS is supported by the NSF and the Heising Simons Foundation. The simulations were performed on resources provided by Sigma2 — the National Infrastructure for High Performance Computing and Data Storage in Norway. Data from the Greenland Ecosystem Monitoring Programme were provided by the Greenland Institute of Natural Resources, Nuuk, Greenland in collaboration with Department of Bioscience, Aarhus University, Denmark.

https://doi.org/10.5194/tc-2022-136
Preprint. Discussion started: 8 July 2022
© Author(s) 2022. CC BY 4.0 License.


References

Åkesson, H., Nisancioglu, K. H., and Nick, F. M.: Impact of Fjord Geometry on Grounding Line Stability, Frontiers in Earth Science, 6, 71, https://doi.org/10.3389/feart.2018.00071, 2018.

Amundson, J. M., Fahnestock, M., Truffer, M., Brown, J., Lüthi, M. P., and Motyka, R. J.: Ice mélange dynamics and implications for terminus stability, Jakobshavn Isbræ, Greenland, Journal of Geophysical Research: Earth Surface, 115, https://doi.org/10.1029/2009JF001405, 2010.

Beaird, N., Straneo, F., and Jenkins, W.: Characteristics of meltwater export from Jakobshavn Isbræ and Ilulissat Icefjord, Annals of Glaciology, 58, 107–117, https://doi.org/10.1017/aog.2017.19, 2017.

Benn, D. I. and Åström, J. A.: Calving glaciers and ice shelves, Advances in Physics: X, 3, 1048–1076, https://doi.org/10.1080/23746149.2018.1513819, 2018.

Bondzio, J. H., Morlighem, M., Seroussi, H., Kleiner, T., Rückamp, M., Mouginot, J., Moon, T., Larour, E. Y., and Humbert, A.: The mechanisms behind Jakobshavn Isbrae's acceleration and mass loss: A 3-D thermomechanical model study, Geophysical Research Letters, 44, 6252–6260, https://doi.org/10.1002/2017GL073309, 2017.

Burton, J. C., Amundson, J. M., Cassotto, R., Kuo, C. C., and Dennin, M.: Quantifying flow and stress in ice mélange, the world's largest granular material, Proceedings of the National Academy of Sciences of the United States of America, 115, 5105–5110, https://doi.org/10.1073/PNAS.1715136115/VIDEO-1, 2018.

Carroll, D., Sutherland, D. A., Hudson, B., Moon, T., Catania, G. A., Shroyer, E. L., Nash, J. D., Bartholomaus, T. C., Felikson, D., Stearns, L. A., Noël, B. P. Y., and van den Broeke, M. R.: The impact of glacier geometry on meltwater plume structure and submarine melt in Greenland fjords, Geophysical Research Letters, 43, 9739–9748, https://doi.org/10.1002/2016GL070170, 2016.

Carroll, D., Sutherland, D. A., Shroyer, E. L., Nash, J. D., Catania, G. A., and Stearns, L. A.: Subglacial discharge-driven renewal of tidewater glacier fjords, Journal of Geophysical Research: Oceans, 122, 6611–6629, https://doi.org/10.1002/2017JC012962, 2017.

Cassotto, R., Fahnestock, M., Amundson, J. M., Truffer, M., and Joughin, I.: Seasonal and interannual variations in ice melange and its impact on terminus stability, Jakobshavn Isbræ, Greenland, Journal of Glaciology, 61, 76–88, https://doi.org/10.3189/2015JoG13J235, 2015.

Cassotto, R., Fahnestock, M., Amundson, J. M., Truffer, M., Boettcher, M. S., De La Peña, S., and Howat, I.: Non-linear glacier response to calving events, Jakobshavn Isbræ, Greenland, Journal of Glaciology, 65, 39–54, https://doi.org/10.1017/JOG.2018.90, 2019.

Catania, G. A., Stearns, L. A., Moon, T. A., Enderlin, E. M., and Jackson, R. H.: Future Evolution of Greenland's Marine-Terminating Outlet Glaciers, Journal of Geophysical Research: Earth Surface, 125, https://doi.org/10.1029/2018JF004873, 2020.

Cavanagh, J. P., Lampkin, D. J., and Moon, T.: Seasonal Variability in Regional Ice Flow Due to Meltwater Injection Into the Shear Margins of Jakobshavn Isbræ, Journal of Geophysical Research: Earth Surface, 122, 2488–2505, https://doi.org/10.1002/2016JF004187, 2017.

Cook, S. J., Christoffersen, P., and Todd, J.: A fully-coupled 3D model of a large Greenlandic outlet glacier with evolving subglacial hydrology, frontal plume melting and calving, Journal of Glaciology, pp. 1–17, https://doi.org/10.1017/jog.2021.109, 2021.

Cowton, T., Slater, D., Sole, A., Goldberg, D., and Nienow, P.: Modeling the impact of glacial runoff on fjord circulation and submarine melt rate using a new subgrid-scale parameterization for glacial plumes, Journal of Geophysical Research: Oceans, 120, 796–812, https://doi.org/10.1002/2014JC010324, 2015.

Cowton, T. R., Todd, J. A., and Benn, D. I.: Sensitivity of Tidewater Glaciers to Submarine Melting Governed by Plume Locations, Geophysical Research Letters, 46, 11 219–11 227, https://doi.org/10.1029/2019GL084215, 2019.

https://doi.org/10.5194/tc-2022-136
Preprint. Discussion started: 8 July 2022
© Author(s) 2022. CC BY 4.0 License.


Cuffey, K. M. and Paterson, W. S. B.: The Physics of Glaciers, Elsevier Science & Technology Books, 4th editio edn., 2010.

Davison, B. J., Cowton, T. R., Cottier, F. R., and Sole, A. J.: Iceberg melting substantially modifies oceanic heat flux towards a major Greenlandic tidewater glacier, Nature Communications, 11, 1–13, https://doi.org/10.1038/s41467-020-19805-7, 2020.

Davison, B. J., Cowton, T., Sole, A., Cottier, F., and Nienow, P.: Modelling the effect of submarine iceberg melting on glacier-adjacent water properties, The Cryosphere, 16, 1181–1196, https://doi.org/10.5194/TC-16-1181-2022, 2022.

De Andrés, E., Slater, D. A., Straneo, F., Otero, J., Das, S., and Navarro, F.: Surface emergence of glacial plumes determined by fjord stratification, Cryosphere, 14, 1951–1969, https://doi.org/10.5194/TC-14-1951-2020, 2020.

Enderlin, E. M., Hamilton, G. S., Straneo, F., and Sutherland, D. A.: Iceberg meltwater fluxes dominate the freshwater budget in Greenland's iceberg-congested glacial fjords, Geophysical Research Letters, 43, 11,287–11,294, https://doi.org/10.1002/2016GL070718, 2016.

Fenty, I., Willis, J., Khazendar, A., Dinardo, S., Forsberg, R., Fukumori, I., Holland, D., Jakobsson, M., Moller, D., Morison, J., Meunchow, A., Rignot, E., Schodlock, M., Thompson, A., Tino, K., Rutherford, M., and Trenholm, N.: Oceans Melting Greenland: Early results from NASA's ocean-ice mission in Greenland, Oceanography, 29, 72–83, https://doi.org/10.5670/ocean.2016.100, 2016.

Fitzmaurice, A., Cenedese, C., and Straneo, F.: A Laboratory Study of Iceberg Side Melting in Vertically Sheared Flows, Journal of Physical Oceanography, 48, 1367–1373, https://doi.org/10.1175/JPO-D-17-0185.1, 2018.

Frank, T., Åkesson, H., de Fleurian, B., Morlighem, M., and Nisancioglu, K.: Geometric Controls of Tidewater Glacier Dynamics, The Cryosphere Discussions, pp. 1–32, https://doi.org/10.5194/TC-2021-81, 2021.

Gladish, C. V., Holland, D. M., Rosing-Asvid, A., Behrens, J. W., and Boje, J.: Oceanic boundary conditions for Jakobshavn Glacier. Part I: Variability and renewal of Ilulissat Icefjord waters, 2001-14, Journal of Physical Oceanography, 45, 3–32, https://doi.org/10.1175/JPO-D-14-0044.1, 2015.

Goelzer, H., Nowicki, S., Payne, A., Larour, E., Seroussi, H., Lipscomb, W. H., Gregory, J., Abe-Ouchi, A., Shepherd, A., Simon, E., Agosta, C., Alexander, P., Aschwanden, A., Barthel, A., Calov, R., Chambers, C., Choi, Y., Cuzzone, J., Dumas, C., Edwards, T., Felikson, D., Fettweis, X., Golledge, N. R., Greve, R., Humbert, A., Huybrechts, P., Le Clec'H, S., Lee, V., Leguy, G., Little, C., Lowry, D., Morlighem, M., Nias, I., Quiquet, A., Rückamp, M., Schlegel, N. J., Slater, D. A., Smith, R., Straneo, F., Tarasov, L., Van De Wal, R., and Van Den Broeke, M.: The future sea-level contribution of the Greenland ice sheet: A multi-model ensemble study of ISMIP6, Cryosphere, 14, 3071–3096, https://doi.org/10.5194/TC-14-3071-2020, 2020.

Greenland Ecosystem Monitoring: MarineBasis Disko - Water column - CTD measurements (Version 1.0) [Data set], Tech. rep., Greenland Ecosystem Monitoring, https://doi.org/https://doi.org/10.17897/WH30-HT61, 2020.

Hager, A. O., Sutherland, D. A., Amundson, J. M., Jackson, R. H., Kienholz, C., Motyka, R. J., and Nash, J. D.: Subglacial Discharge Reflux and Buoyancy Forcing Drive Seasonality in a Silled Glacial Fjord, Journal of Geophysical Research: Oceans, 127, e2021JC018 355, https://doi.org/10.1029/2021JC018355, 2022.

Hughes, K. G.: Pathways, form drag, and turbulence in simulations of an ocean flowing through an ice mélange, Journal of Geophysical Research: Oceans, p. e2021JC018228.

Jackson, R. H., Shroyer, E. L., Nash, J. D., Sutherland, D. A., Carroll, D., Fried, M. J., Catania, G. A., Bartholomaus, T. C., and Stearns, L. A.: Near-glacier surveying of a subglacial discharge plume: Implications for plume parameterizations, Geophysical Research Letters, 44, 6886–6894, https://doi.org/10.1002/2017GL073602, 2017.

Jackson, R. H., Nash, J. D., Kienholz, C., Sutherland, D. A., Amundson, J. M., Motyka, R. J., Winters, D., Skyllingstad, E., and Pettit, E. C.: Meltwater Intrusions Reveal Mechanisms for Rapid Submarine Melt at a Tidewater Glacier, Geophysical Research Letters, 47, e2019GL085 335, https://doi.org/10.1029/2019GL085335, 2020.

https://doi.org/10.5194/tc-2022-136
Preprint. Discussion started: 8 July 2022
© Author(s) 2022. CC BY 4.0 License.

Jenkins, A.: Convection-driven melting near the grounding lines of ice shelves and tidewater glaciers, Journal of Physical Oceanography, 41, 2279–2294, https://doi.org/10.1175/JPO-D-11-03.1, 2011.

Joughin, I., Howat, I. M., Fahnestock, M., Smith, B., Krabill, W., Alley, R. B., Stern, H., and Truffer, M.: Continued evolution of Jakobshavn Isbrae following its rapid speedup, Journal of Geophysical Research, 113, F04 006, https://doi.org/10.1029/2008JF001023, 2008.

Joughin, I., E. Shean, D., E. Smith, B., and Floricioiu, D.: A decade of variability on Jakobshavn Isbræ: Ocean temperatures pace speed through influence on mélange rigidity, Cryosphere, 14, 211–227, https://doi.org/10.5194/TC-14-211-2020, 2020.

Khazendar, A., Fenty, I. G., Carroll, D., Gardner, A., Lee, C. M., Fukumori, I., Wang, O., Zhang, H., Seroussi, H., Moller, D., Noël, B. P. Y., van den Broeke, M. R., Dinardo, S., and Willis, J.: Interruption of two decades of Jakobshavn Isbrae acceleration and thinning as regional ocean cools, Nature Geoscience, 12, 277–283, https://doi.org/10.1038/s41561-019-0329-3, 2019.

Mankoff, K. D., Solgaard, A., Colgan, W., Ahlstrøm, A. P., Abbas Khan, S., and Fausto, R. S.: Greenland Ice Sheet solid ice discharge from 1986 through March 2020, Earth System Science Data, 12, 1367–1383, https://doi.org/10.5194/ESSD-12-1367-2020, 2020.

Marshall, J., Adcroft, A., Hill, C., Perelman, L., and Heisey, C.: A finite-volume, incompressible Navier Stokes model for studies of the ocean on parallel computers, Journal of Geophysical Research: Oceans, 102, 5753–5766, https://doi.org/10.1029/96JC02775, 1997.

Mernild, S. H., Holland, D. M., Holland, D., Rosing-Asvid, A., Yde, J. C., Liston, G. E., and Steffen, K.: Freshwater flux and spatiotemporal simulated runoffvariability into Ilulissat Icefjord, West Greenland, linked to salinity and temperature observations near tidewater glacier margins obtained using instrumented ringed seals, Journal of Physical Oceanography, 45, 1426–1445, https://doi.org/10.1175/JPO-D-14-0217.1, 2015.

Mojica, J. F., Djoumna, G., Holland, D. M., and Holland, D.: Interannual summer mixing processes in the Ilulissat Icefjord, Greenland, Journal of Marine Systems, 214, 103 476, https://doi.org/10.1016/j.jmarsys.2020.103476, 2021.

Moon, T., Sutherland, D. A., Carroll, D., Felikson, D., Kehrl, L., and Straneo, F.: Subsurface iceberg melt key to Greenland fjord freshwater budget, Nature Geoscience, 11, 49–54, https://doi.org/10.1038/s41561-017-0018-z, 2018.

Morlighem, M., Williams, C. N., Rignot, E., An, L., Arndt, J. E., Bamber, J. L., Catania, G., Chauché, N., Dowdeswell, J. A., Dorschel, B., Fenty, I., Hogan, K., Howat, I., Hubbard, A., Jakobsson, M., Jordan, T. M., Kjeldsen, K. K., Millan, R., Mayer, L., Mouginot, J., Noël, B. P. Y., O'Cofaigh, C., Palmer, S., Rysgaard, S., Seroussi, H., Siegert, M. J., Slabon, P., Straneo, F., van den Broeke, M. R., Weinrebe, W., Wood, M., and Zinglersen, K. B.: BedMachine v3: Complete Bed Topography and Ocean Bathymetry Mapping of Greenland From Multibeam Echo Sounding Combined With Mass Conservation, Geophysical Research Letters, 44, 11,051–11,061, https://doi.org/10.1002/2017GL074954, 2017.

Mortensen, J., Rysgaard, S., Bendtsen, J., Lennert, K., Kanzow, T., Lund, H., and Meire, L.: Subglacial Discharge and its Down-Fjord Transformation in West Greenland Fjords With an Ice Melange, Journal of Geophysical Research: Oceans, 125, e2020JC016 301, https://doi.org/10.1029/2020JC016301, 2020.

Motyka, R. J., Truffer, M., Fahnestock, M., Mortensen, J., Rysgaard, S., and Howat, I.: Submarine melting of the 1985 Jakobshavn Isbræ floating tongue and the triggering of the current retreat, Journal of Geophysical Research: Earth Surface, 116, https://doi.org/10.1029/2009JF001632, 2011.

Mouginot, J., Rignot, E., Bjørk, A. A., van den Broeke, M., Millan, R., Morlighem, M., Noël, B., Scheuchl, B., and Wood, M.: Forty-six years of Greenland Ice Sheet mass balance from 1972 to 2018, Proceedings of the National Academy of Sciences of the United States of America, 116, 9239–9244, https://doi.org/https://doi.org/10.1073/pnas.1904242116, 2019.

Muilwijk, M., Straneo, F., Slater, D. A., Smedsrud, L. H., Holte, J., Wood, M., Andresen, C. S., and Harden, B.: Export of ice sheet meltwater from Upernavik Fjord, West Greenland, Journal of Physical Oceanography, -1, https://doi.org/10.1175/JPO-D-21-0084.1, 2021.

https://doi.org/10.5194/tc-2022-136
Preprint. Discussion started: 8 July 2022
© Author(s) 2022. CC BY 4.0 License.


Noël, B., van de Berg, W. J., Lhermitte, S., and van den Broeke, M. R.: Rapid ablation zone expansion amplifies north Greenland mass loss, Science advances, 5, eaaw0123, 2019.

O'Leary, M. and Christoffersen, P.: Calving on tidewater glaciers amplified by submarine frontal melting, Cryosphere, 7, 119–128, https://doi.org/10.5194/TC-7-119-2013, 2013.

Peters, I. R., Amundson, J. M., Cassotto, R., Fahnestock, M., Darnell, K. N., Truffer, M., and Zhang, W. W.: Dynamic jamming of iceberg-choked fjords, Geophysical Research Letters, 42, 1122–1129, https://doi.org/10.1002/2014GL062715, 2015.

Rezvanbehbahani, S., Stearns, L. A., Keramati, R., Shankar, S., and van der Veen, C. J.: Significant contribution of small icebergs to the freshwater budget in Greenland fjords, Communications Earth & Environment, 1, 1–7, https://doi.org/10.1038/s43247-020-00032-3, 2020.

Rignot, E., Fenty, I., Xu, Y., Cai, C., and Kemp, C.: Undercutting of marine-terminating glaciers in West Greenland, Geophysical Research Letters, 42, 5909–5917, https://doi.org/10.1002/2015GL064236, 2015.

Slater, D. A., Goldberg, D. N., Nienow, P. W., and Cowton, T. R.: Scalings for Submarine Melting at Tidewater Glaciers from Buoyant Plume Theory, Journal of Physical Oceanography, 46, 1839–1855, https://doi.org/10.1175/JPO-D-15-0132.1, 2016.

Slater, D. A., Straneo, F., Felikson, D., Little, C. M., Goelzer, H., Fettweis, X., and Holte, J.: Estimating Greenland tidewater glacier retreat driven by submarine melting, Cryosphere, 13, 2489–2509, https://doi.org/10.5194/TC-13-2489-2019, 2019.

Slater, D. A., Benn, D. I., Cowton, T. R., Bassis, J. N., and Todd, J. A.: Calving Multiplier Effect Controlled by Melt Undercut Geometry, Journal of Geophysical Research: Earth Surface, 126, e2021JF006 191, https://doi.org/10.1029/2021JF006191, 2021.

Straneo, F., Sutherland, D. A., Stearns, L., Catania, G., Heimbach, P., Moon, T., Cape, M. R., Laidre, K. L., Barber, D., Rysgaard, S., Mottram, R., Olsen, S., Hopwood, M. J., and Meire, L.: The case for a sustained Greenland Ice sheet-Ocean Observing System (GrIOOS), Frontiers in Marine Science, 6, 138, https://doi.org/https://doi.org/10.3389/fmars.2019.00138, 2019.

Truffer, M. and Motyka, R. J.: Where glaciers meet water: Subaqueous melt and its relevance to glaciers in various settings, Reviews of Geophysics, 54, 220–239, https://doi.org/10.1002/2015RG000494, 2016.

Wood, M., Rignot, E., Fenty, I., An, L., Bjørk, A., van den Broeke, M., Cai, C., Kane, E., Menemenlis, D., Millan, R., Morlighem, M., Mouginot, J., Noël, B., Scheuchl, B., Velicogna, I., Willis, J. K., and Zhang, H.: Ocean forcing drives glacier retreat in Greenland, Science Advances, 7, https://doi.org/DOI: 10.1126/sciadv.aba7282, 2021.